

Including all the lines¹

Robert L. Kurucz

Abstract: I present a progress report on including all the lines in the line lists, including all the lines in the opacities, and including all the lines in the model atmosphere and spectrum synthesis calculations. The increased opacity will improve stellar atmosphere, pulsation, stellar interior, asteroseismology, nova, supernova, and other radiation-hydrodynamics calculations. I also report on producing high-resolution, high-signal-to-noise atlases for use in verifying the line data and spectrum calculations, and as tools for extending laboratory spectrum analyses to higher energy levels. All the data are available on my web site: kurucz.harvard.edu.

PACS Nos: 31.15.ag, 31.30.Gs, 32.30.-r, 32.70.-n, 32.70.Cs, 33.20.-t, 33.70.Ca, 95.30.Ky, 95.75.Fg, 96.60.Fe, 96.60.Ub, 97.10.Ex, 97.10.Tk, 97.60.Bw

Résumé : Je présente un rapport des progrès faits pour inclure toutes les raies dans les listes de raies, incluant toutes les raies dans les opacités et incluant toutes les raies dans les calculs de modèle d'atmosphère et de synthèse de spectre. L'opacité accrue va améliorer les calculs d'atmosphère stellaire, de pulsation, d'intérieur stellaire, d'astéroismologie, de nova et de supernova, ainsi que ceux touchant les autres phénomènes de radiation-hydrodynamique. Je présente aussi un rapport sur la production d'atlas de haute résolution et de haut rapport signal sur bruit à être utilisés dans la vérification des données de raies et les calculs de spectres et comme outils pour étendre les analyses des spectres pris en laboratoire vers des niveaux plus hauts. Toutes les données sont disponibles sur mon site web : kurucz.harvard.edu.

[Traduit par la Rédaction]

1. Introduction

In 1965, I started collecting and computing atomic and molecular line data for computing opacities in model atmospheres and then for synthesizing spectra. I wanted to determine stellar effective temperatures, gravities, and abundances. I still want to.

For 23 years I included more and more lines, but I could never get a solar model to look right, to reproduce the observed energy distribution.

In 1988, I finally produced enough lines, I thought. I completed a calculation of the first 9 ions of the iron group elements, shown in Table 1, using my versions of Cowan's atomic structure programs [1] and the compilation of laboratory energy levels by Sugar and Corliss [2]. There were data for 42 million lines that I combined with data for 1 million lines from my earlier list for lighter and heavier elements, including all the data from the literature. In addition, I had computed line lists for diatomic molecules including 15 million lines of H₂, CH, NH, OH, MgH, SiH, C₂, CN, CO, SiO, and TiO for a total of 58 million lines.

I then tabulated 2 nm resolution opacity distribution functions (ODFs) from the line list for temperatures from 2 000 to 200 000 K and for a range of pressure suitable for stellar atmospheres [3].

Using the ODFs I computed a theoretical solar model [4] with the solar effective temperature and gravity, the current

solar abundances from [5], mixing-length to scale-height ratio $\text{L}/\text{H} = 1.25$, and constant microturbulent velocity 1.5 km s^{-1} . It generally matched the observed energy distribution from [6].

I computed thousands of model atmospheres that I distributed on magnetic tapes, then on CDs, and now on my web site, kurucz.harvard.edu. They made observers happy. However, agreement with low-resolution observations of integrated properties does not imply correctness.

2. Problems

In 1988 the abundances were wrong, the microturbulent velocity was wrong, the convection was wrong, and the opacities were wrong.

Since 1965 the Fe abundance has varied by over a factor of 10. In 1988 the Fe abundance was 1.66 times larger than today. There was mixing-length convection with an exaggerated, constant microturbulent velocity. In the grids of models, the default microturbulent velocity was 2 km s^{-1} . My 1D models still have mixing-length convection, but now with a depth-dependent microturbulent velocity that scales with the convective velocity. 3D models with cellular convection do not have microturbulent velocity at all but use the doppler shifts from the convective motions.

In 1988 the line opacity was underestimated, because not enough lines were included in the line lists. Table 2 is an outline for the Fe II line calculation at that time. The higher

Received 28 September 2010. Accepted 9 November 2010. Published at www.nrcresearchpress.com/cjp on 6 May 2011.

R.L. Kurucz. Harvard-Smithsonian Center for Astrophysics, Cambridge, MA 02138, USA.

E-mail for correspondence: rkurucz@cfa.harvard.edu

¹This article is part of a Special Issue on the 10th International Colloquium on Atomic Spectra and Oscillator Strengths for Astrophysical and Laboratory Plasmas.

Table 1. Iron group lines computed at San Diego supercomputer center 1988.

	I	II	III	IV	V	VI	VII	VIII	IX
Ca	48 573	4 227	11 740	113 121	330 004	217 929	125 560	30 156	22 803
Sc	191 253	49 811	1 578	16 985	130 563	456 400	227 121	136 916	30 587
Ti	867 399	264 867	23 742	5 079	37 610	155 919	356 808	230 705	139 356
V	1 156 790	925 330	284 003	61 630	8 427	39 525	160 652	443 343	231 753
Cr	434 773	1 304 043	990 951	366 851	73 222	10 886	39 668	164 228	454 312
Mn	327 741	878 996	1 589 314	1 033 926	450 293	79 068	14 024	39 770	147 442
Fe	789 176	1 264 969	1 604 934	1 776 984	1 008 385	475 750	90 250	14 561	39 346
Co	546 130	1 048 188	2 198 940	1 569 347	2 032 402	1 089 039	562 192	88 976	15 185
Ni	149 926	404 556	1 309 729	1 918 070	1 971 819	2 211 919	967 466	602 486	79 627

Table 2. Fe II in 1988 based on [7] and on [2].

Even: 22 configurations; 5723 levels; 354 known levels; 729 Hamiltonian parameters, all CI; 46 free LS parameters; standard deviation 142 cm⁻¹

d ⁷					
d ⁶ s	d ⁵ s ²	d ⁶ 4d	d ⁵ 4s4d	d ⁴ 4s ² 4d	d ⁵ 4p ²
d ⁶ s	d ⁵ 4s5s	d ⁵ 5d	d ⁵ 4s5d	d ⁶ 5g	
d ⁶ s	d ⁵ 4s6s	d ⁶ 6d	d ⁵ 4s6d	d ⁶ 6g	
d ⁶ 7s		d ⁶ 7d		d ⁶ 7g	
d ⁶ 8s		d ⁶ 8d			
d ⁶ 9s					
Odd: 16 configurations; 5198 levels; 435 known levels; 541 Hamiltonian parameters, all CI; 43 free LS parameters; standard deviation 135 cm ⁻¹					
d ⁶ 4p	d ⁵ 4s4p	d ⁶ 4f	d ⁵ 4s4f	d ⁴ 4s ² 4p	
d ⁶ 5p	d ⁵ 4s5p	d ⁶ 5f			
d ⁶ 6p	d ⁵ 4s6p	d ⁶ 6f			
d ⁶ 7p	d ⁵ 4s7p				
d ⁶ 8p	d ⁵ 4s8p				
d ⁶ 9p					
Total E1 lines saved		1 254 969			
E1 lines with good wavelengths		45 815			

energy levels that produce series of lines that merge into ultraviolet (UV) continua were not included. Those levels also produce huge numbers of weaker lines in the visible and infrared (IR) that blend and fill in the spaces between the stronger lines. Also, lines of heavier elements were not systematically included. Moreover, the additional broadening from hyperfine and isotopic splitting was not included.

In 1988 the opacities were low but were balanced by high abundances that made the lines stronger and by high microturbulent velocity that made the lines broader. Now, the abundances, the convection, and the opacities are still wrong, but they have improved. I am concentrating on filling out the line lists.

3. Examples of new calculations

In Tables 3 to 5 I show sample statistics from my new semi-empirical calculations for Fe II, Ni I, and Co I to illustrate how important it is to do the basic physics well and how much data there are to deal with. Ni, Co, and Fe are prominent in supernovae, including both radioactive and stable isotopes. There is not space here for the lifetime and gf comparisons. Generally, low configurations that have been well studied in the laboratory produce good lifetimes and gf values, while higher configurations that are poorly observed

and are strongly mixed are not well constrained in least-squares fits and necessarily produce poorer results and large scatter. My hope is that the predicted energy levels can help the laboratory spectroscopists to identify more levels and further constrain the least-squares fits. From my side, I check the computed gf values in spectrum calculations by comparing with observed spectra. I adjust the gf values so that the spectra match. Then I search for patterns in the adjustments that suggest corrections in the least-squares fits.

As the new calculations accumulate I put on my web site the output files of the least-squares fits to the energy levels, energy level tables, with E and J, identification, strongest eigenvector components, lifetime, A-sum, C₄, C₆, Landé g. The sums are complete up to the first ($n = 10$) energy level not included. There are electric dipole (E1), magnetic dipole (M1), and electric quadrupole (E2) line lists. Radiative, Stark, and van der Waals damping constants and Landé g values are automatically produced for each line. Branching fractions are also computed. Hyperfine and isotopic splitting are included when the data exist, but not automatically. Eigenvalues are replaced by measured energies, so that lines connecting measured levels have correct wavelengths. Most of the lines have uncertain wavelengths, because they connect predicted rather than measured levels. Laboratory measurements of gf values and lifetimes will be included. Measured or estimated widths of auto-ionizing levels will be included when available. The partition function is tabulated for a range of densities.

When computations with the necessary information are available from other workers, I am happy to use those data instead of repeating the work.

Once the line list for an ion or molecule is validated it will be incorporated into the wavelength sorted line lists on my web site for computing opacities or detailed spectra. The web directories are located at kurucz.harvard.edu/atoms.html and kurucz.harvard.edu/molecules.html for the details, and kurucz.harvard.edu/linelists.html for the completed line lists.

Table 6 presents line statistics from some of my recent calculations that show an order of magnitude increase over my earlier work, because I am treating about 3 times as many levels. Considering only the ions in the table, there are about 257 million lines compared to 26 million in the 1988 calculation. Table 7 shows my estimate (individual ions only to astronomical accuracy) that my line lists will have several billion atomic and molecular lines if I can continue my work. I expect to update and replace all my previous calculations for lighter elements and for the iron group in the near future. Then I will concentrate on extending the work to heavier elements and higher ions.

Table 3. Fe II based on [2, 7–14].

Even: 46 configurations; 19771 levels; 421 known levels; 2645 Hamiltonian parameters, all CI; 48 free LS parameters; standard deviation 48 cm ⁻¹							
d ⁶ s	d ⁵ s ²	d ⁶ 4d	d ⁵ 4s4d			d ⁴ s ² 4d	d ⁵ 4p ²
d ⁶ 5s	d ⁵ 4s5s	d ⁶ 5d	d ⁵ 4s5d	d ⁶ 5g	d ⁵ 4s5g	d ⁴ s ² 5s	
d ⁶ 6s	d ⁵ 4s6s	d ⁶ 6d	d ⁵ 4s6d	d ⁶ 6g	d ⁵ 4s6g		
d ⁶ 7s	d ⁵ 4s7s	d ⁶ 7d	d ⁵ 4s7d	d ⁶ 7g	d ⁵ 4s7g	d ⁶ 7i	d ⁵ 4s7i
d ⁶ 8s	d ⁵ 4s8s	d ⁶ 8d	d ⁵ 4s8d	d ⁶ 8g	d ⁵ 4s8g	d ⁶ 8i	d ⁵ 4s8i
d ⁶ 9s	d ⁵ 4s9s	d ⁶ 9d	d ⁵ 4s9d	d ⁶ 9g	d ⁵ 4s9g	d ⁶ 9i	d ⁵ 4s9i
Odd: 39 configurations; 19652 levels; 596 known levels; 2996 Hamiltonian parameters, all CI; 48 free LS parameters; standard deviation 64 cm ⁻¹							
d ⁶ 4p	d ⁵ 4s4p	d ⁶ 4f	d ⁵ 4s4f			d ⁴ s ² 4p	d ⁴ -s ² 4f
d ⁶ 5p	d ⁵ 4s5p	d ⁶ 5f	d ⁵ 4s5f			d ⁴ s ² 5p	
d ⁶ 6p	d ⁵ 4s6p	d ⁶ 6f	d ⁵ 4s6f	d ⁶ 6h	d ⁵ 4s6h		
d ⁶ 7p	d ⁵ 4s7p	d ⁶ 7f	d ⁵ 4s7f	d ⁶ 7h	d ⁵ 4s7h		
d ⁶ 8p	d ⁵ 4s8p	d ⁶ 8f	d ⁵ 4s8f	d ⁶ 8h	d ⁵ 4s8h	d ⁶ 8k	d ⁵ 4s8k
d ⁶ 9p	d ⁵ 4s9p	d ⁶ 9f	d ⁵ 4s9f	d ⁶ 9h	d ⁵ 4s9h	d ⁶ 9k	d ⁵ 4s9k
Total E1 lines saved				7 615 097 new	1 254 969 old	ratio = 6.1	
E1 lines with good wavelengths				103 357 new	45 815 old	ratio = 2.3	
Forbidden lines	M1 even	M1 odd		E2 even	E2 odd		
Total lines saved	2 707 590	3 665 949		10 861 275	13 550 604		
With good wavelengths	38 256	66 961		59 008	110 668		
Between metastable	1232	0		1827	0		
Isotope	⁵⁴ Fe	⁵⁵ Fe	⁵⁶ Fe	⁵⁷ Fe	⁵⁸ Fe	⁵⁹ Fe	⁶⁰ Fe
Fraction	0.059	0.0	0.9172	0.021	0.0028	0.0	0.0

Note: ⁵⁷Fe has not yet been measured, because it has hyperfine splitting. Rosberg et al. [15] have measured ⁵⁶Fe–⁵⁴Fe in 9 lines and ⁵⁸Fe–⁵⁶Fe in one line. I split the computed lines by hand. The data from these papers after Sugar and Corliss [2] are not in the NIST atomic energy level database.

Table 4. Ni I based on Litzén et al. [16] with isotopic splitting.

Total E1 lines saved		732 160 new	149 926 old	ratio = 4.9
E1 lines with good wavelengths		9663 new	3949 old	ratio = 2.4
Isotope	⁵⁶ Ni	⁵⁷ Ni	⁵⁸ Ni	⁵⁹ Ni
Fraction	0.0	0.0	0.6827	0.0
			⁶⁰ Ni	⁶¹ Ni
				⁶² Ni
				⁶³ Ni
				⁶⁴ Ni

Note: There are measured isotopic splittings for 326 lines from which I determined 131 energy levels relative to the ground. These levels are connected by **11670 isotopic lines**. Hyperfine splitting was included for ⁶¹Ni, but only 6 levels have been measured, which produce 4 lines with 38 components. A pure isotope laboratory analysis is needed. Ni I lines are asymmetric from the splitting and they now agree in shape with lines in the solar spectrum.

Table 5. Co I based on Pickering and Thorne [17] and on Pickering [18] with hyperfine splitting.

Total E1 lines saved		3 771 908 new	546 130 old	ratio = 6.9
E1 lines with good wavelengths		15 441 new	9 879 old	ratio = 2.4
Isotope	⁵⁶ Co	⁵⁷ Co	⁵⁸ Co	⁵⁹ Co
Fraction	0.0	1.	0.0	0.0
			⁶⁰ Co	
				0.0

Note: Hyperfine constants have been measured in 297 levels, which produce **244264 component E1 lines**. The new calculation greatly improves the appearance of the Co I lines in the solar spectrum.

4. TiO and H₂O

These are examples of incorporating data from other researchers.

Schwenke [19] calculated energy levels for TiO, including in the Hamiltonian the 20 lowest vibration states of the 13 lowest electronic states of TiO (singlets a, b, c, d, f, g, h and

triplets X, A, B, C, D, E) and their interactions. He determined parameters by fitting the observed energies or by computing theoretical values. Using Langhoff's [20] transition moments, Schwenke generated a line list for J=0 to 300 for the isotopologues ⁴⁶Ti¹⁶O, ⁴⁷Ti¹⁶O, ⁴⁸Ti¹⁶O, ⁴⁹Ti¹⁶O, and ⁵⁰Ti¹⁶O with fractional abundances 0.080, 0.073, 0.738, 0.055, and 0.054. My version has 37 744 499 lines.

Table 6. Sample recent atomic calculations.

	Config.		Levels		E1 lines		
	Even	Odd	Even	Odd	Good wl	Total	Old
S I	61	61	2 161	2 270	24 722	225 605	
Sc I	61	61	2 014	2 318	15 546	737 992	191 253
Sc II	61	61	509	644	3 436	116 491	49 811
Sc V	49	54	1 317	1 021	2 180	645 368	130 563
Ti I	61	61	6 628	7 350	33 815	4 758 992	867 399
Ti II	61	61	2 096	2 318	8 188	835 027	264 867
Ti III	73	68	3 636	3 845	4 090	499 739	23 742
V I	61	61	13 767	15 952	23 342	7 043 556	1 156 790
V II	61	61	6 740	7 422	18 389	3 932 853	925 330
V III	61	61	2 094	2 318	9 892	966 528	284 003
Cr I	47	40	18 842	18 660	35 315	2 582 957	434 773
Cr II	61	61	13 767	15 890	58 996	6 970 052	1 304 043
Cr III	61	61	6 580	7 526	23 150	5 535 931	990 951
Mn I	44	39	18 343	19 652	16 798	1 481 464	327 741
Mn II	50	41	19 686	19 870	31 437	4 523 390	878 996
Mn III	61	61	13 706	15 890	17 294	10 525 088	1 589 314
Fe I	61	50	18 655	18 850	93 508	6 029 023	789 176
Fe II	46	39	19 771	19 652	103 357	7 615 097	1 264 969
Fe III	49	41	19 720	19 820	37 199	9 548 787	1 604 934
Fe IV	61	54	13 767	14 211	8 408	14 617 228	1 776 984
Fe V	61	61	6 560	7 526	11 417	7 785 320	1 008 385
Fe VI	73	73	2 094	2 496	3 534	9 072 714	475 750
Fe VII	85	86	7 132	7 032	2 326	2 816 992	90 250
Fe VIII	52	52	1 365	1 244	233	220 166	14 561
Co I	61	61	10 920	13 085	15 441	3 771 900	546 130
Co II	61	50	18 655	19 364	23 355	10 050 728	1 361 114
Co III	44	39	18 343	19 652	9 356	11 515 139	2 198 940
Ni I	61	61	4 303	5 758	9 663	732 160	149 925
Ni II	61	61	10 270	11 429	55 590	3 645 991	404 556
Ni III	61	50	18 655	19 364	21 251	11 120 833	1 309 729
Ni IV	44	39	18 343	19 517	5 659	15 152 636	1 918 070
Ni V	46	41	10 637	19 238	10 637	15 622 452	1 971 819
Ni VI	61	61	13 706	15 792	12 219	17 971 672	2 211 919
Ni VII	73	73	24 756	19 567	3 502	28 328 012	967 466
Ni VIII	73	73	12 714	8 903	758	12 308 126	602 486
Ni IX	85	86	7 132	7 032	253	2 671 345	79 627
Ni X	52	52	1 365	1 208	235	285 029	
Cu I	61	61	920	1 260	5 720	28 112	
Cu II	61	61	4 303	5 758	14 959	622 985	
Cu IV	55	50	9 563	17 365	9 563	11 857 712	
Cu X	85	86	508	3 002	159	2 910 966	
Y I	61	61	1 634	2 141	5 393	59 226	

Note: Total new / total old = 257 million / 28 million = 10.

Good analyses and a similar semi-empirical treatment are needed for CaOH, ScO, VO, YO, ZrO, LaO, etc.

Partridge and Schwenke [21] treated H₂O semi-empirically. They included isotopologues H₂¹⁶O, H₂¹⁷O, H₂¹⁸O, and HD¹⁶O. My version has 65 912 356 lines. I hope to obtain a newer line list with a billion lines in the near future.

5. Computing opacity

My program DFSYNTHETHE [22] can compute the LTE opacity spectrum of 1 billion lines, at 4 million frequencies, for 1200 T-P pairs, for a range of Vturb, on a workstation.

Those spectra can be statistically processed into ODF tables

as they are computed, or treated in some other approximation, or they can be saved directly. Instead of dealing with lines, one can just interpolate (and doppler shift) the opacity spectra. The wavelength range can be limited to treat individual filters or echelle orders. One can pretabulate an opacity spectrum for each element, or group of elements that vary together, and then scale the spectra to the desired abundances and add them to produce the total opacity spectrum for those abundances.

6. Model atmosphere programs

My model atmosphere program ATLAS12 [23] can deal with 1 billion lines by sampling. It preselects into a smaller

Table 7. Estimated lines in 3d and 4d group sequences (in millions).

	I	II	III	IV	V	VI	VII	VIII	IX	X	...
Ca	0.05										
Sc	0.7	0.05									
Ti	5	0.7	0.05								
V	14	5	0.7	0.05							
Cr	10	14	5	0.7	0.05						
Mn	1.5	10	14	5	0.7	0.05					
Fe	6	7	10	14	5	0.7	0.05				
Co	4	10	7	10	14	5	0.7	0.05			
Ni	0.7	4	10	7	10	14	5	0.7	0.05		
Cu	0.03	0.6	4	10	7	10	14	5	0.7	0.05	
Zn	0.1	0.03	0.6	4	10	7	10	14	5	0.7	...
Ga		0.1	0.03	0.6	4	10	7	10	14	5	...
Ge			0.1	0.03	0.6	4	10	7	10	14	...
As				0.1	0.03	0.6	4	10	7	10	...
Se					0.1	0.03	0.6	4	10	7	...
Br						0.1	0.03	0.6	4	10	...
Kr							0.1	0.03	0.6	4	...
Rb								0.1	0.03	0.6	...
Sr	0.05								0.1	0.03	...
Y	0.7	0.05								0.1	...
Zr	5	0.7	0.05								
Nb	14	5	0.7	0.05							
Mo	10	14	5	0.7	0.05						
Tc	1.5	10	14	5	0.7	0.05					
Ru	6	7	10	14	5	0.7	0.05				
Rh	4	10	7	10	14	5	0.7	0.05			
Pd	0.7	4	10	7	10	14	5	0.7	0.05		
Ag	0.03	0.6	4	10	7	10	14	5	0.7	0.05	
Cd	0.1	0.03	0.6	4	10	7	10	14	5	0.7	...
In		0.1	0.03	0.6	4	10	7	10	14	5	...
Sn			0.1	0.03	0.6	4	10	7	10	14	...
Sb				0.1	0.03	0.6	4	10	7	10	...
Te					0.1	0.03	0.6	4	10	7	...
I						0.1	0.03	0.6	4	10	...
Xe							0.1	0.03	0.6	4	...
Cs								0.1	0.03	0.6	...
Ba									0.1	0.03	...

Note: Total 3d > 500 million; total 4d > 500 million; + lanthanide sequences > 1000 million; + all the other element sequences.

line list the lines that are relevant for the model. It defaults to 30 000 sampling points, but it could sample a million. It can treat arbitrary depth-dependent abundances and velocities.

My program ATLAS9 [24] uses ODFs, so it is independent of the number of lines.

7. Atlases and spectrum synthesis

High-resolution, high signal-to-noise spectra are needed to test the line data and the spectrum synthesis programs and to determine the stellar parameters.

There are no high-quality solar spectra taken above the atmosphere in the UV, visible, or IR out to 2.2 μm . There is a recent central intensity atlas produced with an FTS on the ACE satellite [25] that covers from 2.2 to 14 μm . I will fit the intensity spectrum by adjusting the line parameters, and then I will compute the irradiance spectrum with those line data.

In the UV, there are not even “good” quality solar spectra. There are various good quality solar spectra taken through

the atmosphere in the visible and IR. I have been trying to reduce the FTS spectra taken by James Brault from Kitt Peak to produce central intensity, limb intensity, flux, and irradiance atlases.

Figure 1 shows the Kitt Peak flux atlas [26] for 300 to 1000 nm with resolving power greater than 300 000 and signal-to-noise greater than 3000. Figure 2 is the telluric absorption in the flux atlas. Most of the line data come from the HITRAN database [27]. Figure 3 is the Kitt Peak irradiance atlas [28] derived from the flux spectrum by removing the telluric lines. Figure 4 shows a section of a similarly constructed irradiance atlas [29] in the H band from 1580 to 1740 and in the K band from 1920 to 2100 nm that I will extend.

Line data can be tested by comparing calculated spectra to the atlases. Figure 5 shows a sample spectrum calculation with the lines labelled for a nearly empty angstrom of the solar flux atlas shown in Fig. 1. It shows the quality of the observed FTS spectrum from Kitt Peak, the computed telluric

Fig. 1. Kitt Peak solar flux atlas [26].

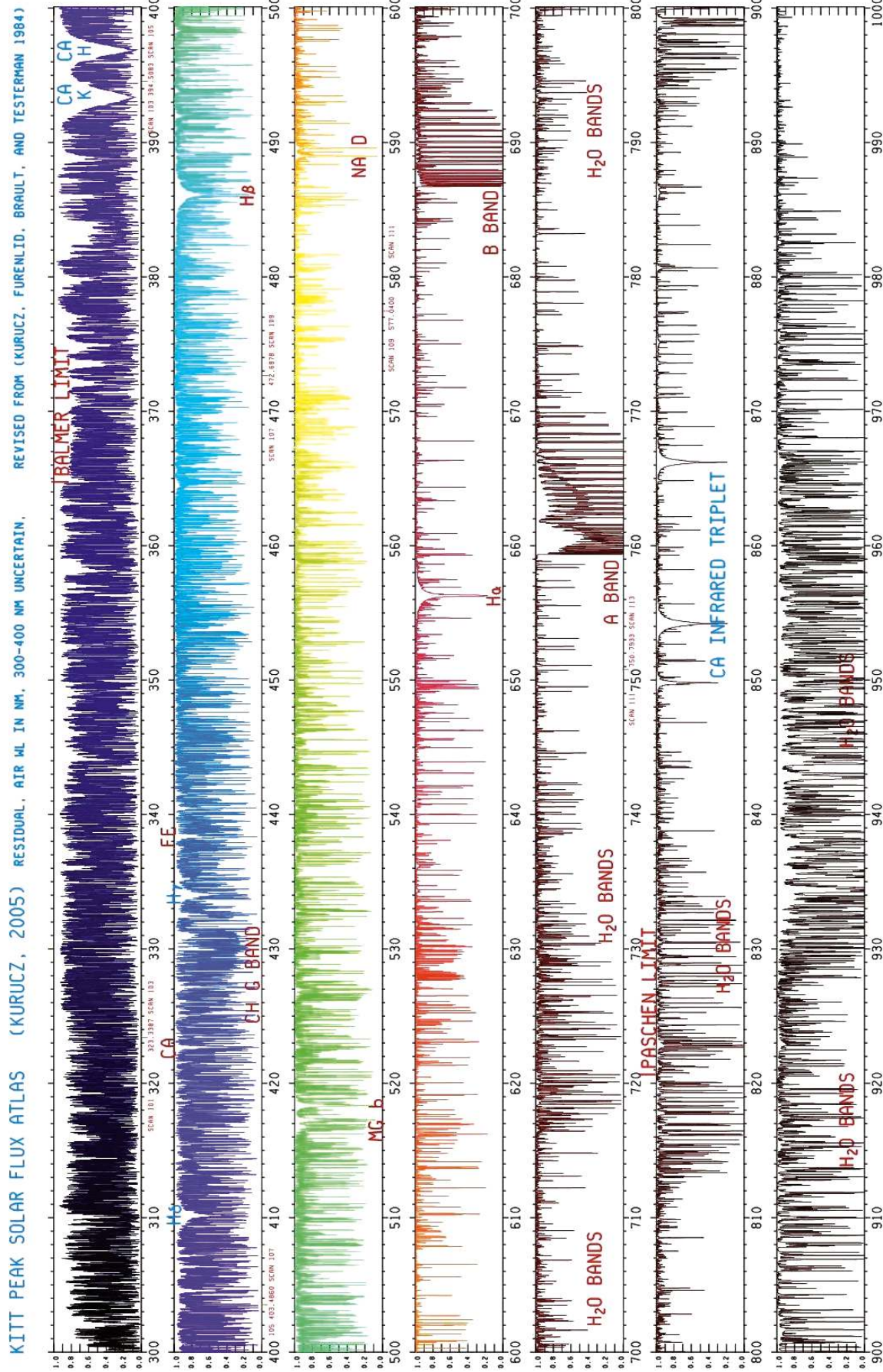


Fig. 2. Telluric lines in Kitt Peak solar flux atlas, Fig. 1.

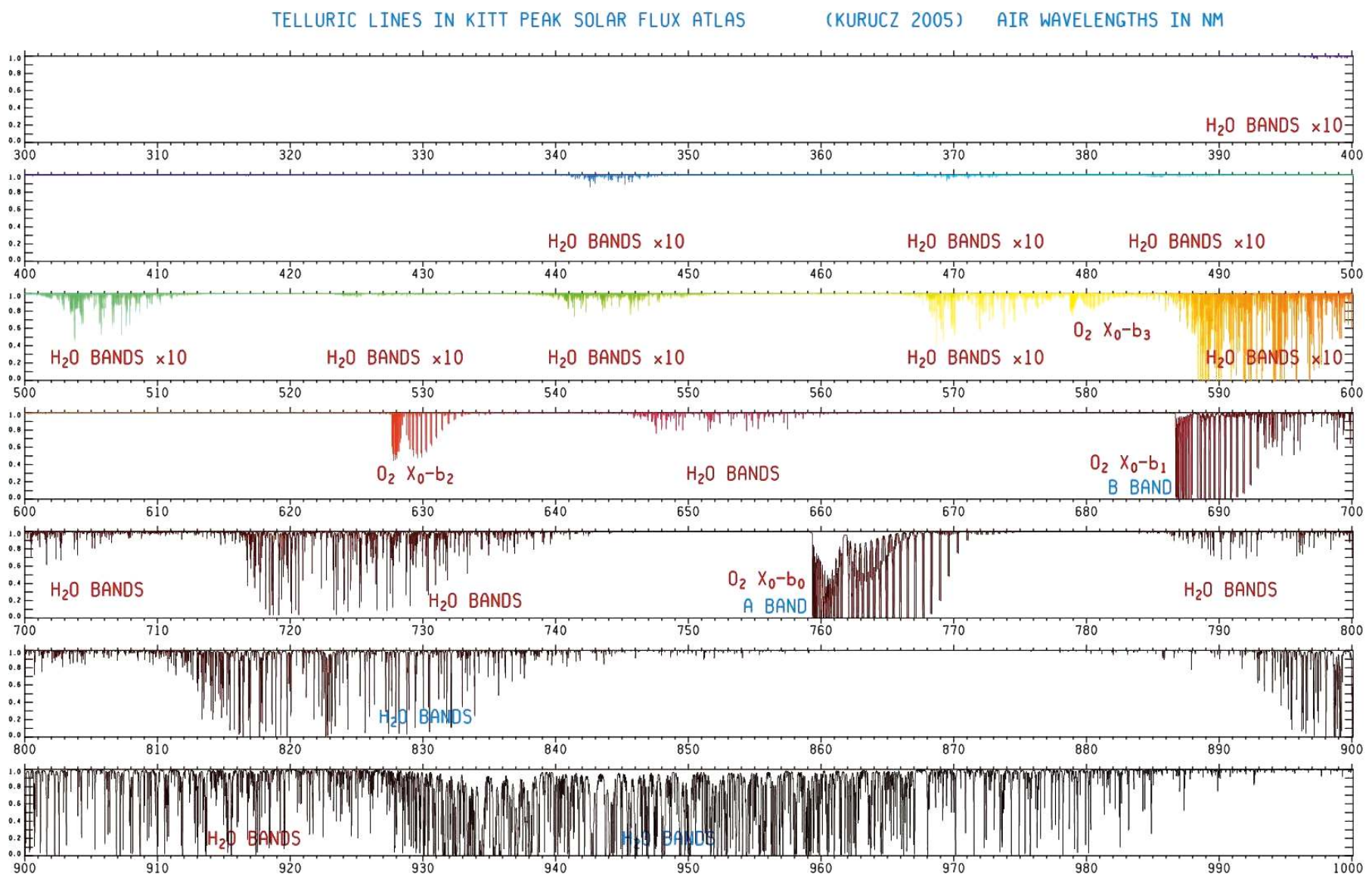


Fig. 3. Kitt Peak irradiance atlas [28].

KITT PEAK IRRADIANCE ATLAS (KURUCZ 2005) RESIDUAL, VACUUM WAVELENGTHS IN NM, 300–400 NM UNTIL

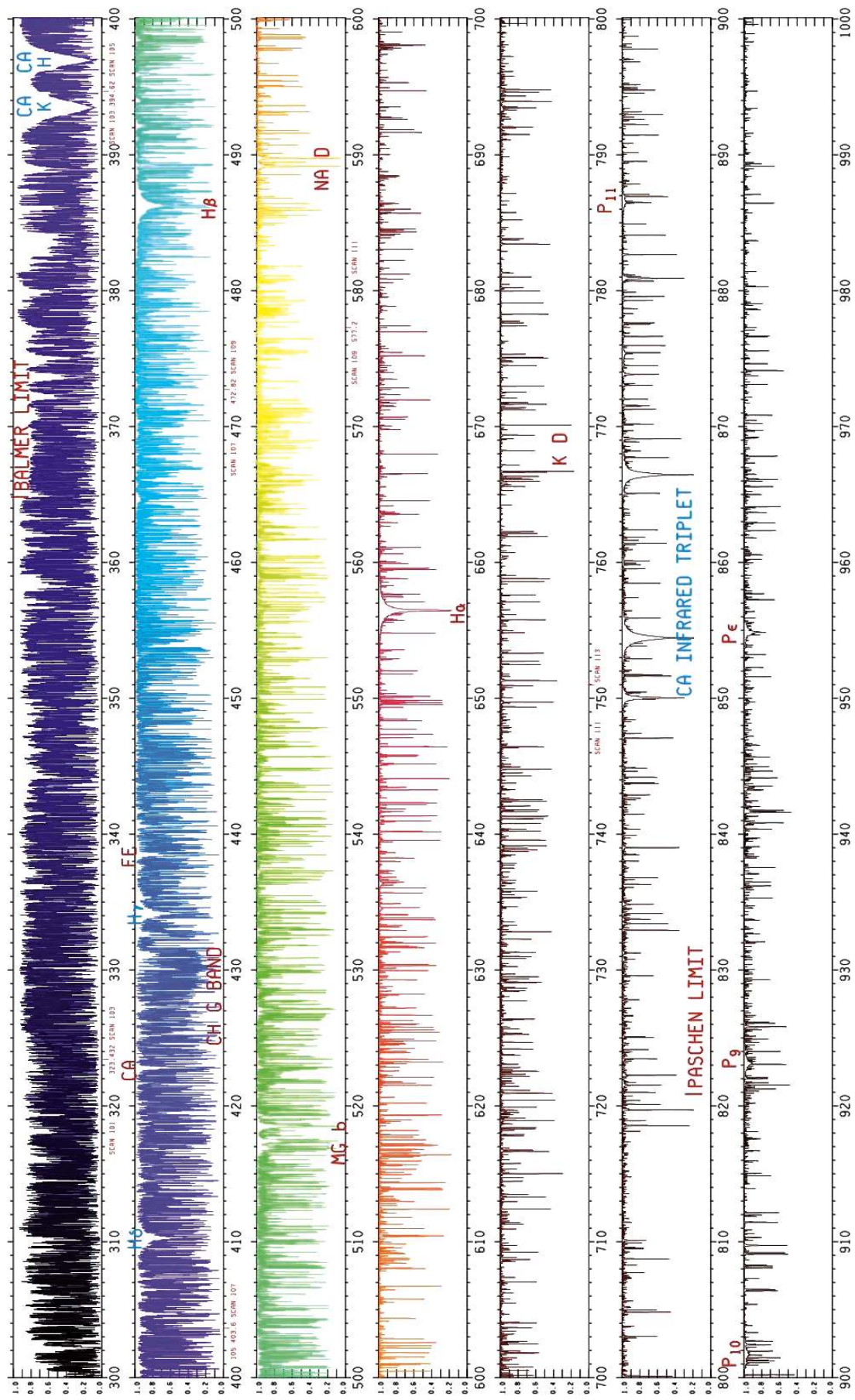
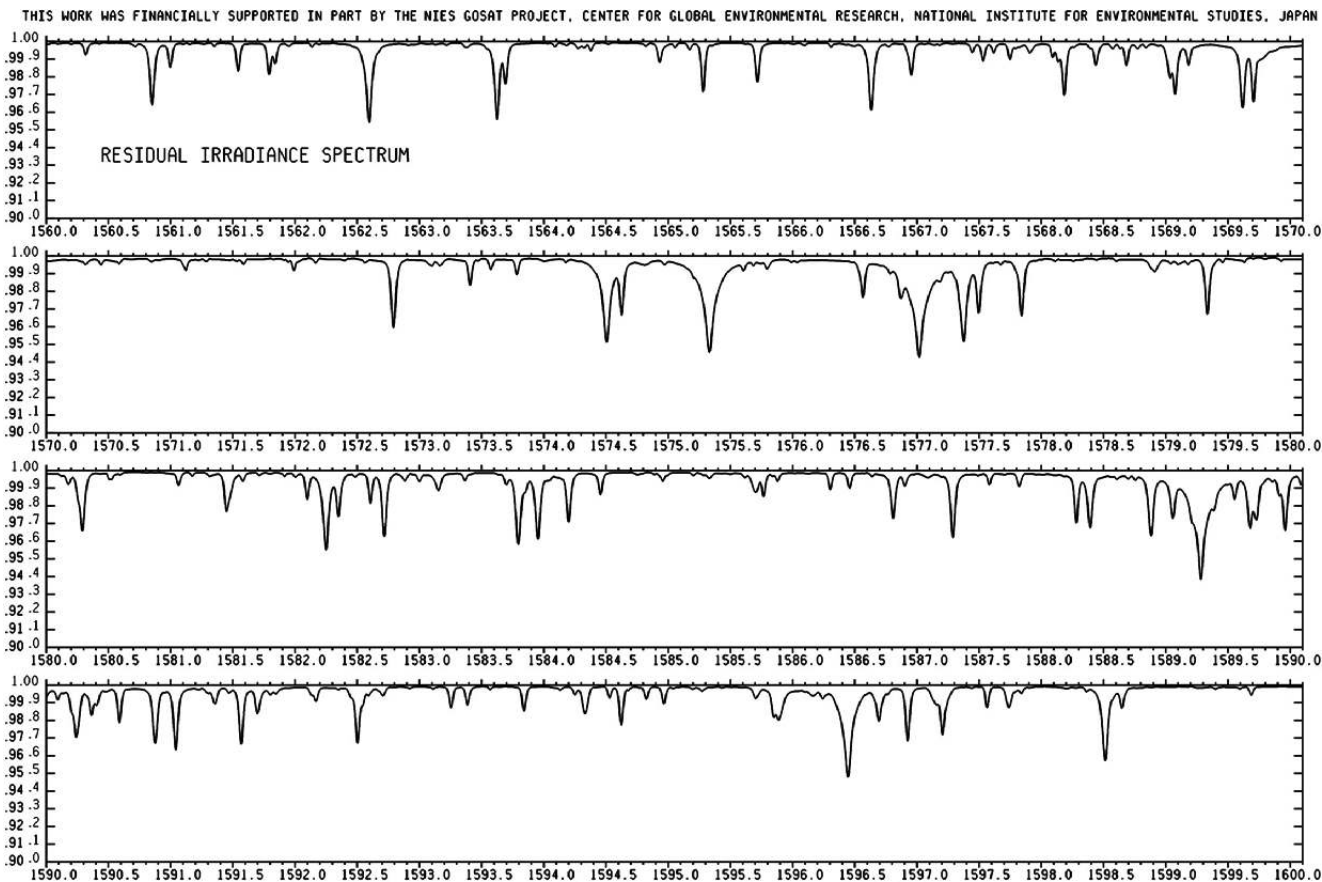


Fig. 4. Partial irradiance atlas in H and K bands [29]. Thus far, 1560–1740 nm in H and 1920–2100 nm in K have been completed.



spectrum, the computed solar spectrum, and the computed FTS spectrum for Kitt Peak. Complicated blends, missing lines, and hyperfine splitting are obvious.

From my experience synthesizing spectra and working with high-quality atlases of the sun and other stars, I have come to the following conclusions:

- Abundances are generally determined from blended features that must be deconvolved by synthesizing the features including every significant blending line.
- One half the discernible lines in the sun are missing from the lists of lines with good wavelengths. Every line has to be adjusted in wavelength, damping constants, and gf value.
- Most lines used in abundance analyses are not suitable. The systematic errors tend to result in overestimates of abundances. Including many lines reduces the accuracy because of the systematic errors.
- We do not know anything with certainty about the sun, except its mass.

8. Spectrum analysis using stellar atlases as the laboratory source

Chemically peculiar or CP stars are early type stars with large over- and under-abundances. They can have very small projected rotation velocities, hence narrow lines. HR6000 has Teff 13450K, $\log g = 4.3$, and projected rotation velocity about 1.5 km s^{-1} from [30]. The abundances (log relative to solar) are Fe [+0.9], Xe [+4.6], P [> +1.5], Ti [+0.55], Cr

[+0.2], Mn [+1.5], Y [+1.2], Hg [+2.7], and He, C, N, O, Al, Mg, Si, S, Cl, Sc, V, Co, Ni, and Sr under-abundant. With initial guidance from Johansson, Castelli analyzed the Fe II lines and has determined 126 new 4d, 5d, 6d, and 4f energy levels [12–14]. These levels produce more than 18 000 lines throughout the spectrum from UV to IR. Figure 6 shows the improvement between Fe II computed with the 2008 Kurucz line list and the current line list. Figure 7 shows the improvement in the spectrum including all the lines. Note that many lines are still missing and remain to be identified. Hubrig has obtained IR spectra with the CRIRES spectrograph on the VLT telescope to extend the analysis.

In stars, these Fe lines are seen in absorption and the Boltzmann factor for the lower level determines the line strength. Laboratory sources in emission have to populate the upper level. These lines appear in more “normal” stars as well but are smeared out and blended by rotation velocities 10 to 100 times higher.

Considerable telescope time should be allocated to making high-resolution, high signal-to-noise atlases in the UV, visible, and IR of selected CP stars. These would be used as tools for extending laboratory spectrum analyses to higher energy levels for as many elements as possible. Of course, high-quality solar atlases have been used to extend laboratory analyses for as long as they have existed (cf [31, 32]).

9. Conclusion

The inclusion of heavier elements, higher stages of ioniza-

Fig. 5. Sample calculation that compares synthetic spectra to the flux spectrum at 599.1 nm in Fig. 1. Each spectrum is plotted twice, at normal scale, and at 10 times scale to emphasize discrepancies. The observed FTS spectrum is plotted in black. The computed telluric spectrum broadened to the FTS resolution is plotted in cyan. The computed solar spectrum broadened to the FTS resolution is plotted in red. The product of the solar and telluric spectra broadened to the FTS resolution is plotted in magenta. Comparing the magenta spectrum with the black spectrum tests the wavelengths, gf values, and damping constants. (The labels are described in the caption to Fig. 7.) The left feature at 599.13 with depth 0.26 is mainly Fe II, with some blending with CN, Fe I, Yb II, and telluric H₂O. The right feature at 599.185 with depth 0.05 is mostly 15 hyperfine components of a Co I line, overlaid by a telluric H₂O line. There are also blends with CN, Cr I, and Ca I. There are missing lines in both wings; several beyond 599.21. There are probably additional missing lines included in both features.

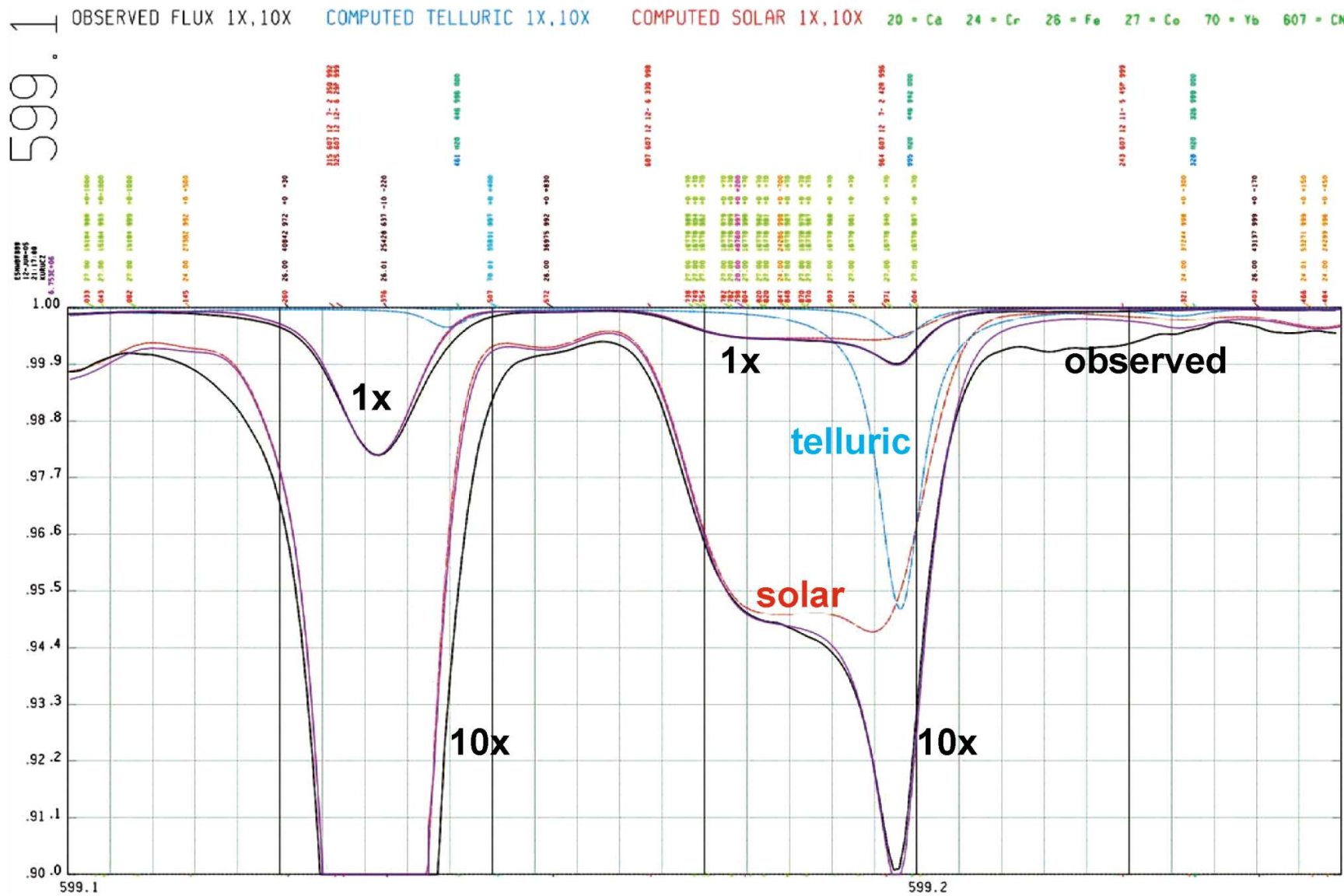


Fig. 6. The upper panel shows the Fe II spectrum computed for HR6000 (Teff = 12450K, log g = 4.3, vsini = 1.5 km s⁻¹, Fe = [+0.9]) using Kurucz data as of 2008. The lower panel is the same calculation using the current Kurucz Fe II line list.

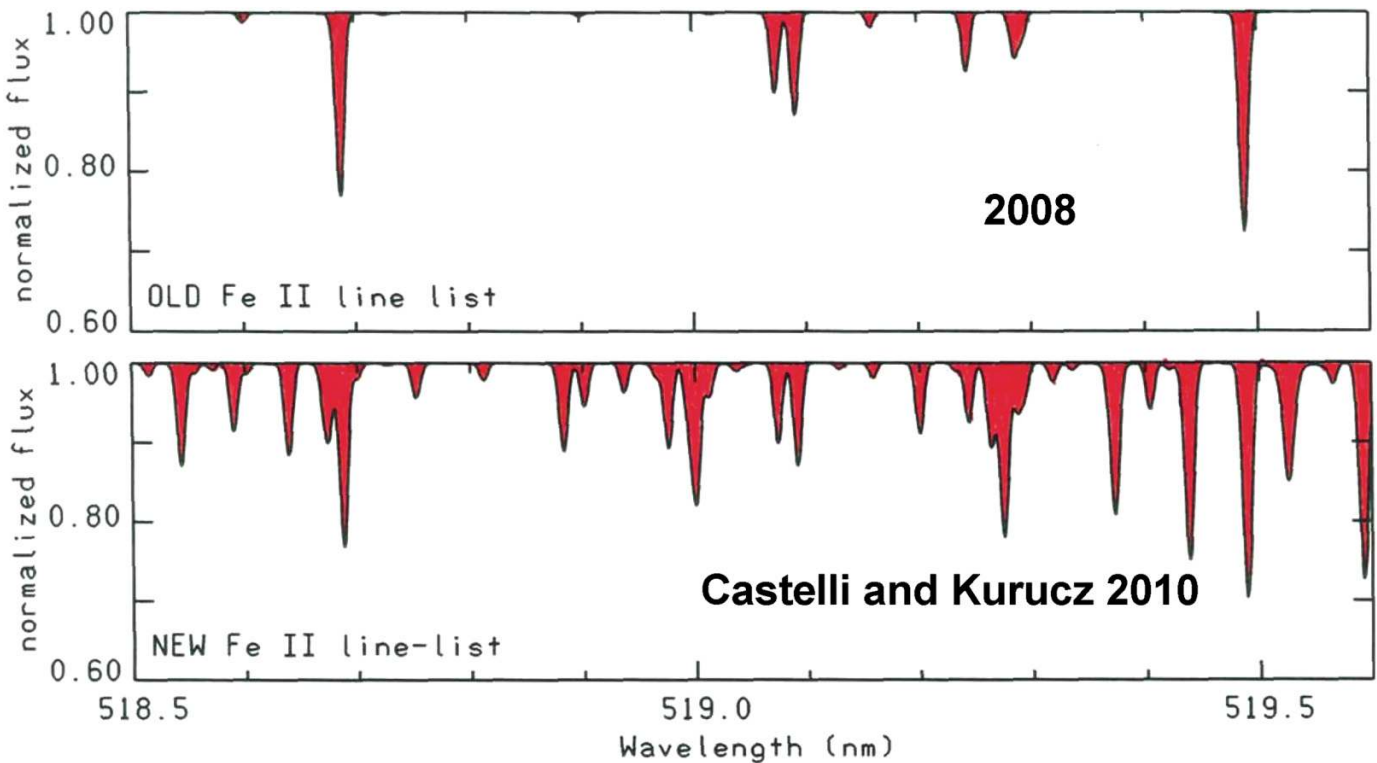
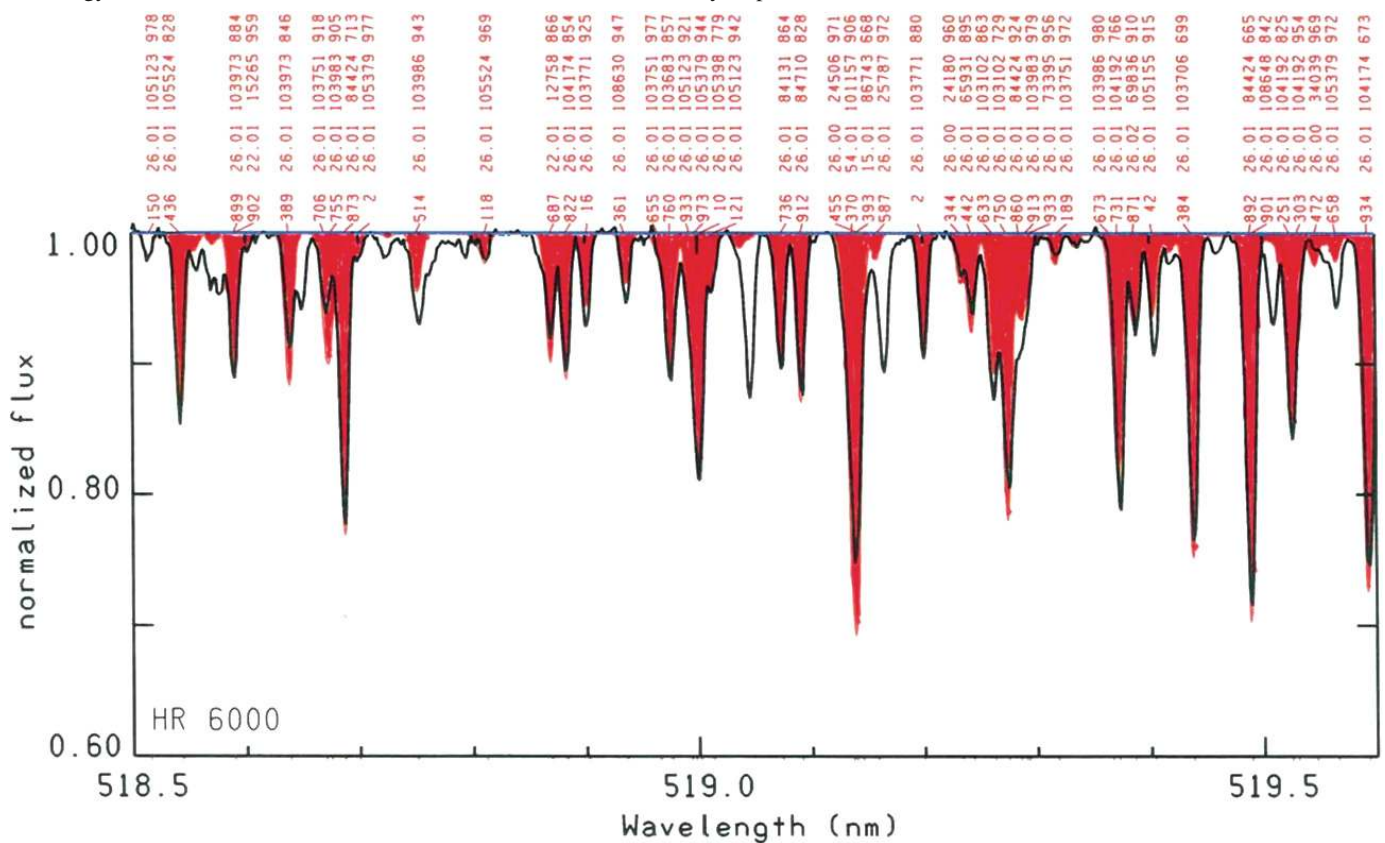


Fig. 7. The synthetic spectrum (in red) computed with a line list including the new Fe II lines compared to the observed spectrum of HR6000 (in black). Note that many lines are missing and remain to be identified. The line identifications can be decoded as follows: for the first line, 150 = last 3 digits of the wavelength 518.5150; 26 = atomic number of Fe; 0.01 = charge/100, i.e., 26.01 identifies the line as Fe II; 195123 is the energy of the lower level in cm⁻¹; 970 is the residual central intensity in per mil.



tion, additional molecules, and higher energy levels will increase the opacity in stellar atmosphere, pulsation, stellar interior, asteroseismology, nova, supernova, and other radiation hydrodynamics calculations. Detailed and more complete line lists will allow more accurate interpretation of features in spectra and the more accurate determination of stellar properties at any level from elementary 1D approximations to the most sophisticated 3D time-dependent treatments.

References

1. R.L. Kurucz. *In Transactions of the International Astronomical Union, XXB*. Edited by M. McNally. Kluwer, Dordrecht. 1988. p. 168.
2. J. Sugar and C. Corliss. *J. Phys. Chem. Ref. Data*, **14**, Suppl. 2, 664 (1985).
3. R.L. Kurucz. *Rev. Mex. Astron. Astrofis.* **23**, 181 (1992).
4. R.L. Kurucz. *Stellar populations of galaxies*. Edited by B. Barbuy and A. Renzini. Kluwer, Dordrecht, Netherlands. 1992. p. 225.
5. E. Anders and N. Grevesse. *Geochim. Cosmochim. Acta*, **53**, 197 (1989). doi:10.1016/0016-7037(89)90286-X.
6. H. Neckel and D. Labs. *Sol. Phys.* **90**, 205 (1984). doi:10.1007/BF00173953.
7. S. Johansson. *Phys. Scr.* **18**, 217 (1978). doi:10.1088/0031-8949/18/4/004.
8. J. Adam, B. Baschek, S. Johansson, A.E. Nilsson, and T. Brage. *Astrophys. J.* **312**, 337 (1987). doi:10.1086/164878.
9. S. Johansson and B. Baschek. *Nucl. Instrum. Methods Phys. Res., Sect. B*, **31**, 222 (1988). doi:10.1016/0168-583X(88)90420-X.
10. M. Rosberg and S. Johansson. *Phys. Scr.* **45**, 590 (1992). doi:10.1088/0031-8949/45/6/009.
11. E. Biémont, S. Johansson, and P. Palmeri. *Phys. Scr.* **55**, 559 (1997). doi:10.1088/0031-8949/55/5/008.
12. F. Castelli, S. Johansson, and S. Hubrig. *J. Phys. Conf. Ser.* **130**, 012003 (2008). doi:10.1088/1742-6596/130/1/012003.
13. F. Castelli, R.L. Kurucz, and S. Hubrig. *Astron. Astrophys.* **508**, 401 (2009). doi:10.1051/0004-6361/200912518.
14. F. Castelli and R.L. Kurucz. *Astron. Astrophys.* **520**, A57 (2010). doi:10.1051/0004-6361/201015126.
15. M. Rosberg, U. Litzén, and S. Johansson. *Mon. Not. R. Astron. Soc.* **262**, L1 (1993).
16. U. Litzén, J.W. Brault, and A.P. Thorne. *Phys. Scr.* **47**, 628 (1993). doi:10.1088/0031-8949/47/5/004.
17. J.C. Pickering and A.P. Thorne. *Astrophys. J.* **107**, Suppl., 761 (1996). doi:10.1086/192381.
18. J.C. Pickering. *Astrophys. J.* **107**, Suppl., 811 (1996). doi:10.1086/192382.
19. D.W. Schwenke. *Faraday Discuss.* **109**, 321 (1998). doi:10.1039/a800070k.
20. S.R. Langhoff. *Astrophys. J.* **481**, 1007 (1997). doi:10.1086/304077.
21. H. Partridge and D.W. Schwenke. *J. Chem. Phys.* **106**, 4618 (1997). doi:10.1063/1.473987.
22. R.L. Kurucz. *Mem. Soc. Astron. Ital.* **8**, Suppl., 72 (2005).
23. R.L. Kurucz. *In Peculiar versus normal phenomena in A-type and related stars*. Edited by M.M. Dworetsky, F. Castelli, and R. Faraggiana. *Astr. Soc. Pacific Conf. Ser.* **44**, 87 (1993).
24. R.L. Kurucz. ATLAS9 Stellar atmosphere programs and 2 km/s grid. Kurucz CD-ROM No.13. Cambridge, Mass.: Smithsonian Astrophysical Observatory. 1993.
25. F. Hase, L. Wallace, S.D. McLeod, J.J. Harrison, and P.F. Bernath. *J. Quant. Spectrosc. Radiat. Transf.* **111**, 521 (2010). doi:10.1016/j.jqsrt.2009.10.020.
26. R.L. Kurucz. Kitt Peak Solar Flux Atlas. 2005. Available from kurucz.harvard.edu/sun/fluxatlas2005.
27. L.S. Rothman, D. Jacquemart, A. Barbe, D. Chris Benner, M. Birk, L.R. Brown, M.R. Carleer, C. Chackerian, Jr, K. Chance, and L. Coudert. *J. Quant. Spectrosc. Radiat. Transf.* **96**, 139 (2005). doi:10.1016/j.jqsrt.2004.10.008.
28. R.L. Kurucz. Kitt Peak Solar Irradiance Atlas (2005). Available from kurucz.harvard.edu/sun/irradiance2005.
29. R.L. Kurucz. Irradiance in the H and K bands (2008). Available from kurucz.harvard.edu/sun/irradiance2008.
30. F. Castelli and S. Hubrig. *Astron. Astrophys.* **475**, 1041 (2007). doi:10.1051/0004-6361:20077923.
31. M. Geller. A high-resolution atlas of the infrared spectrum of the sun and earth atmosphere from space. Vol. III. Key to identification of solar features. NASA Reference Pub. 1224, Vol. III. 1992. pp. 456.
32. P.F. Bernath and R. Colin. *J. Mol. Spectrosc.* **257**, 20 (2009). doi:10.1016/j.jms.2009.06.003.